# Appendix C
# Multiple Ray Path Separation Altitudes

We develop the expressions for the differences in altitudes of the ray path tangency points between the multiple rays generated by the Case A, Case B, and Case C scenarios. We begin with Case C.

## C.1 Case C: A Discontinuous Lapse Rate

Figure 2-7(d) shows the multipath relationship between $h$ and $h_{\mathrm{LG}}$, which results from a discontinuous lapse rate with the appropriate polarity. Differential expressions for the altitude differences between these multiple rays at their tangency points with the Earth's limb can be estimated for Case C from the power series expansion for $\delta\alpha(r_*) = \alpha(r_*) - \alpha^+(r_*) = (\alpha(r_*) - \alpha^-(r_*)) + (\alpha^-(r_*) - \alpha^+(r_*))$. From Eqs. (2.3-21), (2.3-23), and (2.3.31) with $K_\gamma = 3/8$, we have for $r_* \le r_o$

$$\delta\alpha(r) = -\left(\Delta\gamma H_{p_o}\right)\alpha^-(r_*)\left(\frac{2}{\sqrt{\pi}}\sigma - \frac{3}{2}\sigma^2 + \frac{4}{\sqrt{\pi}}\sigma^3 - 2\sigma^4 + \cdots\right) \qquad \text{(C-1)}$$

where $\sigma$ is given by $\sigma^2 = \left(r_o - r_*\right)/H_{p_o}$. From the thin-screen model given by Eq. (2.2-5), we have

$$h_{\mathrm{LG}} - h_{\mathrm{LG}}(1) \doteq h - h_o - D\left[\alpha(r_*) - \alpha\left(r_o\right) + \delta\alpha(r_*)\right] \qquad \text{(C-2)}$$

We expand $\alpha\left(r_o\right)$ about $r_*$ and define $\xi(r_*)$ by the relation

$$\left.\begin{aligned} \xi(r_*) &= \zeta(r_*)\alpha(r_*)\frac{D}{H_{p_o}}\left(\Delta\gamma H_{p_o}\right) \\ \zeta(r_*) &= \left(1+\frac{D}{H_{p_o}}\alpha(r_*)\right)^{-1} \end{aligned}\right\} \tag{C-3}$$

The quantity $\xi$ has a value of approximately $5\Delta\gamma$ (i.e., small) for nominal conditions at the tropopause. Truncating terms in Eq. (C-1) above a quadratic in $\sigma$, one obtains

$$\sigma = \frac{\xi}{\sqrt{\pi}\left(1+3\xi/2\right)} \pm \sqrt{\frac{\xi^2}{\pi\left(1+3\xi/2\right)^2} - \frac{\left[h_{\mathrm{LG}} - h_{\mathrm{LG}}(1)\right]\zeta}{\left(1+3\xi/2\right)H_{p_o}}} + \cdots \tag{C-4}$$

Since $\sigma \geq 0$, it follows that Eq. (C-4) admits solutions only when $\xi > 0$; that is, caustics occur only when $\Delta\gamma > 0$. When $h_{\mathrm{LG}} = h_{\mathrm{LG}}(1)$, the altitude in $h_{\mathrm{LG}}$-space of maximum ray path separation, we obtain from Eq. (C-4) the two roots

$$\left.\begin{aligned} \sigma &= 0 \\ \sigma &= \frac{2\xi}{\sqrt{\pi}\left(1+3\xi/2\right)} \end{aligned}\right\} \tag{C-5}$$

Since $\xi$ is small, truncation in Eq. (C-1) to $\sigma^2$ terms is valid, and Eq. (C-4) should be fairly accurate in the neighborhood of the caustic zone. Equation (C-5) yields the maximum altitude separation, which occurs when $h_{\mathrm{LG}} = h_{\mathrm{LG}}(1)$, of

$$\frac{h_o - h^-(1)}{H_{p_o}} = \frac{4\xi^2}{\pi\left(1+3\xi/2\right)^2} + \mathrm{O}\left[\xi^3\right] \tag{C-6}$$

To obtain the spread in Doppler between the corresponding two tones, one would multiply Eq. (C-6) by the factor $\dot{h}_{\mathrm{LG}} H_{p_o} / (\lambda D)$.

When $h_{\mathrm{LG}} = h_{\mathrm{LG}}(2)$, which is where $dh / dh_{\mathrm{LG}} \to \infty$, Eq. (C-4) has but one root, and

$$\frac{h_o - h^-(2)}{H_{p_o}} = \frac{\xi^2}{\pi\left(1+3\xi/2\right)^2} + \mathrm{O}\left[\xi^3\right] \tag{C-7}$$

This marks the first contact point with the caustic surface and the epoch of onset of the multiple rays. The ratio $dh / dh_{\mathrm{LG}}$ is the defocusing factor. Thus,

$$\frac{dh^+}{dh_{\mathrm{LG}}} = \zeta \tag{C-8}$$

It follows that the nominal upper altitude at the onset of ray path separation is given by

$$\frac{h^+(2) - h_o}{H_{p_o}} \cong \zeta \frac{h_{\mathrm{LG}}(2) - h_{\mathrm{LG}}(1)}{H_{p_o}} = \frac{\xi^2}{\pi\left(1 + 3\xi/2\right)} \; + \; \mathrm{O}\left[\xi^3\right] \tag{C-9}$$

Adding Eqs. (C-7) and (C-9) yields the separation in altitudes between the nominal upper ray and the lower ray at the onset of ray path separation, and multiplying this sum by $\dot{h}_{\mathrm{LG}} H_{p_o} / (\lambda D)$ yields the Doppler spread. If this Doppler spread is well outside the first Fresnel zone, then distinct tones should appear in a power spectrum (see Fig. 1-11); if not, a diffraction treatment is required. In any case, a diffraction treatment (or at least a third-order ray optics approach) is required in the neighborhood of the point where $dh / dh_{\mathrm{LG}} \to \infty$ (see Appendix D). Equation (2.4-1) also can be applied to obtain the phase offsets between the multiple rays. The ray path separation scale varies essentially quadratically with $\Delta\gamma$.

## C.2 Case B: A Discontinuous Scale Height

From Eqs. (2.3-21) and (2.3-30), we obtain $\delta\alpha(r_*) = \alpha(r_*) - \alpha^+(r_*)$ for the case of a discontinuous scale height at $r = r_o$:

$$\delta\alpha(r_*) = \frac{\Delta H_{p_o}}{H_{p_o}} \alpha^-\left(r_o\right)\left[\frac{2\sigma}{\sqrt{\pi}} - \sigma^2 + \; \cdots\right], \; r_* \le r_o \tag{C-10}$$

Defining $\eta(r_*)$ by

$$\left.\begin{aligned} \eta(r_*) &= -(1-\zeta)\frac{\Delta H_{p_o}}{H_{p_o}} \\ \zeta(r_*) &= \left(1 + \frac{D}{H_{p_o}}\alpha(r_*)\right)^{-1} \end{aligned}\right\} \tag{C-11}$$

and solving for $\sigma$, we obtain

$$\sigma = \frac{\eta}{\sqrt{\pi}(1+\eta)} \pm \sqrt{\frac{\eta^2}{\pi(1+\eta)^2} - \frac{\left(h_{\mathrm{LG}} - h_{\mathrm{LG}}(1)\right)\zeta}{(1+\eta)H_{p_o}}} + \cdots \tag{C-12}$$

from which the relative altitudes of the multiple ray paths may be obtained as in Case C. Since $\sigma > 0$, it follows that $\Delta H_{p_o}$ must be negative to obtain a caustic surface. The multipath separation scales quadratically with $\Delta H_{p_o} / H_{p_o}$.

## C.3 Case A: A Discontinuous Refractivity

An abrupt discontinuity in an exponentially varying background refractivity, $\Delta N$, can be treated by following an approach similar to that taken for the other cases. It can be shown from Eqs. (2.2-5) and (A-49) that we need the roots of the equation

$$0 = \sigma^2 \zeta^{-1} + \left(\frac{D}{H_{p_o}}\right)\left(\alpha_o^+ + \left(\frac{2}{\sqrt{\pi}}\right)\left(\alpha_o^- \sigma - \alpha_o^+ \sqrt{\sigma^2 - \kappa}\right) + \Delta\alpha_S\right) + \frac{h_{LG} - h_o}{H_{p_o}} + O[\sigma^3] \tag{C-13a}$$

If one expands the Snell and radical parts and drops small terms, one obtains an alternate form:

$$\left.\begin{aligned} &\sigma^2 \zeta^{-1} + 2\frac{g}{\sqrt{1-\beta}}\sigma + \left(\frac{D}{H_{p_o}}\right)\alpha_o^+ + \frac{g}{\sigma} + \frac{h_{LG} - h_o}{H_{p_o}} \doteq 0 \\ &g = -\Delta N_o \left(\frac{D}{H_{p_o}}\right)\left(\frac{2r_o}{H_{p_o}}\right)^{1/2} \end{aligned}\right\} \tag{C-13b}$$

When $dh_{LG} / dh = 0$, it follows that the condition

$$\sigma^3 \zeta^{-1} + \frac{g\sigma}{(1-\beta)^{1/2}} - \frac{g}{2} \doteq 0 \tag{C-14}$$

defines the value of $\sigma(2)$ and also $h_{LG}(2)$ and $h(2)$, the first contact point with the caustic. Equation (C-14) has but one root for $g > 0$. That root is given to good approximation by the form

$$\sigma(2) \doteq \left(\frac{g\zeta}{2}\right)^{1/3} \tag{C-15}$$

Therefore, $h_o - h(2)$ grows approximately as $(-\Delta N_o)^{2/3}$ when $\Delta N_o < 0$.

To obtain the maximum separation, we set $h_{LG} = h_{LG}(1) = h_o - D\left[\alpha^+(r_o) + \Delta\alpha(r_o)_S\right]$ and solve for the roots in Eq. (C-13a). It can be shown from Eq. (C-13b) that one obtains the approximate expression

$$\sigma^3\zeta^{-1} + 2g\frac{2g}{(1-\beta)^{1/2}}\sigma^2 - 2\sqrt{-\Delta N_o}\,\frac{D}{H_{p_o}}\sigma + g \doteq 0 \qquad \text{(C-16)}$$

which yields the upper root for $\sigma(1)$ and, therefore, an estimate for the maximum separation in altitude, $h_o - h(1)$. Except for small values of $-\Delta N_o / N_o$, a higher-degree expansion is required for accuracy. It is better to use Eqs. (2.2-5) and (A-49) without expanding in a power series.

The separation altitude at onset of multipath (first contact point), the maximum altitude separation (where the main branch terminates), and the width of the shadow zone are shown in Fig. C-1, which is based on a numerical integration of Eq. (2.2-2). The low Earth orbiting (LEO) satellite's orbit radius is $r_{\mathrm{L}} = 1.1 r_o$. Because of the higher ambient refractivity and lower altitude, this

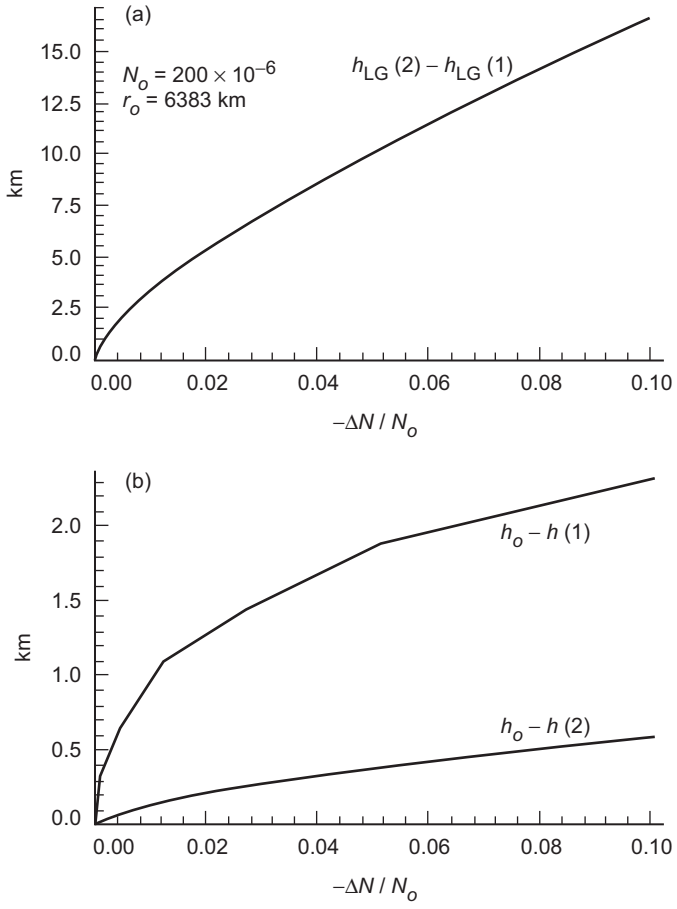


**Fig. C-1. Altitude separations and shadow zone width for Case A: (a) width of shadow zone and (b) altitude separation of ray path tangency points.**

example would be more applicable to a water vapor layer in the lower troposphere. Here the abscissa is the fractional change $-\Delta N_o / N_o$ across the boundary for the case where $\Delta N_o < 0$, and, therefore, the case where both a shadow zone and a caustic are encountered below the boundary surface. The maximum multipath ($h_o - h(1)$) separation altitude at the tangency points of the rays scales approximately as $(-\Delta N_o)^{1/3}$; the length of the shadow zone scales roughly as $(-\Delta N_o)^{2/3}$ at the boundary.

For a positive $\Delta N_o$, one obtains a doublet ray without a caustic and without a shadow zone. This can be visualized by flipping about the horizontal axis (at $h_{\mathrm{LG}}$) the ray path altitude branch in Fig. 2-7(a). Both the cases $\Delta N_o < 0$ and $\Delta N_o > 0$ are shown in Fig. C-2, which provides the $(h_{\mathrm{LG}}, h)$ relationship for these cases. A Fresnel treatment of these cases is shown in Fig. 2-11. When $\Delta N_o > 0$, interference effects are seen several seconds before the main ray hits the boundary. An estimate of the offset of this earlier epoch where multipath first commences—corresponding to $t_1$ in Fig. 2-2(a)—is given by

$$\Delta t = \frac{D}{V_\perp} \Delta \alpha_{\mathrm{S}} \tag{C-17}$$

For the example shown in Fig. C-2 ($\Delta N_o / N_o = +0.05$), this would result in an initiation of multipath interference about 10 s earlier, that is, when the main ray is still $\zeta^+(r_o) V_\perp \Delta t$, or about 5 km *above* the boundary, which is well outside

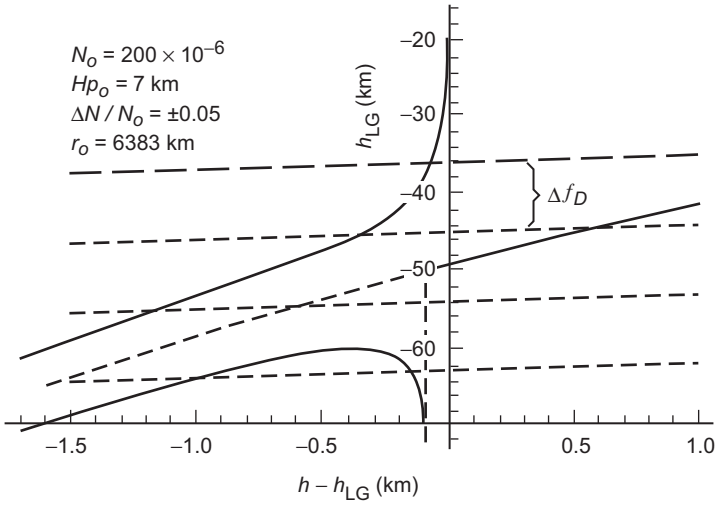


**Fig. C-2. Case A example of multipath altitudes and Doppler tones for both a positive and negative discontinuity in refractivity at $r_o$.**

the first Fresnel zone. The interference would be slight at first because of the severe defocusing just below the boundary.

The nearly horizontal dashed lines in Fig. C-2 are constant Doppler contours. The separation between contours ranges between ~30 Hz and ~45 Hz depending on the obliquity between the propagation plane and the LEO orbit plane. For the $\Delta N / N = -0.05$ curve, no stationary phase paths exist with turning point values in the range $r_o - 64\ \mathrm{m} < r_* \le r_o$, resulting also in a shadow zone. Fresnel diffraction for this case is shown in Fig. 2-11. The Mie scattering version for this case is given in Chapter 3, Fig. 3-25. There it is shown that the shadow zone corresponds to a region where no stationary phase points exist in the scattering series representation over spectral number space.